ChemPubSoc Europe

DOI: 10.1002/celc.201402193

Fundamental Properties of Phenylboronic-Acid-Coated Gate Field-Effect Transistor for Saccharide Sensing

Taira Kajisa and Toshiya Sakata*[a]

We report the surface and electrical characteristics of a phenylboronic acid (PBA)-coated gate field effect transistor (FET) biosensor for a highly sensitive detection of various saccharides. 4-mercaptophenylboronic acid (MPBA) was self-assembled on a Au extended-gate electrode, which was used as a saccharide recognition substrate of the PBA–FET. The binding affinity of PBA with various monosaccharides and disaccharides were evaluated by the amount of voltage changes on the Au gate surface in response to sugar concentrations using the PBA–FET. The specific diol-binding of PBA with saccharides induces molecular charges onto PBA, resulting in the detection of charges at a lower concentration of 50 μM. In particular, the binding affinities of PBA with the saccharides contributes to the different electrical signals. The platform based on the PBA–FET is useful for a convenient and highly sensitive detection of various saccharides in the fields of food engineering and medicine.

1. Introduction

Saccharides are important constituents and play an important role of vital activity for all living organisms in nutrition, metabolism, and immunity. Monosaccharides, starting with glucose, fructose and galactose, are absorbed in the body as the final decomposed product in a metabolism. Therefore, the control of sugar concentrations in a body is meaningful from both the perspectives of nutritional healthcare and diagnostic medical care, such as diabetes mellitus. In addition, it has been proved that polysaccharides, which are synthesized as diverse sugar chains, play an important role for the intra- and intercellular signaling transduction and the cell–cell recognition from the viewpoint of glycotechnology in the recent years.[1] Also in the food engineering field the interest in not only natural sugars but also artificial sweeteners are increasing in terms of food safety and health trends. Moreover, it is known that the concentration of nucleotide sugars such as inosinic acid, which is a kind of "Umami", is closely related to food quality.[2] From these backgrounds, a novel detection technique of saccharides at a higher sensitivity is desirable in the fields of clinical diagnosis, food industry, and biochemistry.

In the present state, glucose sensors, saccharimeters, K-value assays and so on are used as conventional saccharide sensors, where enzymatic,[3] electrochemical,[4] chromatographic detection methods have been developed.[5] Among them, an enzymatic glucose sensor is a typical and prevailing saccharide sensor because of its high sensitivity and selectivity. Enzymatic glucose detection has the advantage that a sugar can bind to the enzyme specifically even in biological fluids such as blood and urine. However, there are still plenty of room for improving intermediates such as the glucose oxidase redox system, enzymatic stability, and limitation of sensitivity. From these reason, non-enzymatic saccharide sensors have been studied and developed in the field of analytical technology.[6]

Phenylboronic acid (PBA) and its derivatives have been mainly applied in non-enzymatic biosensing systems substituting for enzymatic saccharide sensors. PBA can reversibly bind to saccharides and polyols, so that the reaction had been analyzed by various techniques, such as spectrometric absorption,[7] fluorescence,[8] circular dichroism,[9] and optical methods.[10] The equilibrium of PBA based on diol binding with saccharides is indicated by Scheme 1.[11] When the diol group in

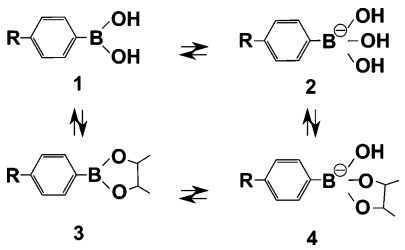

Scheme 1. Equilibrium between the phenylboronic acid derivative and the diol.

a substrate interacts with PBA, the boron atom, which forms nonionic and electron-deficient states with tertiary structure, is changed into a boron anion composed of an electron-rich state with quarternary structure. Detection of glucose using PBA derivatives has been much reported, and there has also

[a] *Dr. T. Kajisa, Prof. T. Sakata*
Department of Materials Science and Engineering
Graduate School of Engineering
The University of Tokyo, 7-3-1 Hongo
Bunkyo-ku, Tokyo 113-8656 (Japan)
Tel: +81-3-5841-1842
E-mail: sakata@biofet.t.u-tokyo.ac.jp

been some reports about the affinity of PBA with various sugars. Springsteen and Wang calculated the binding constants between PBA and various saccharides from changes in the fluorescent intensity, which were obtained by the competition method in sample solutions containing Arizarin Red S, although the binding affinity of the fluorescent dye may be different from that of most saccharides.[12]

A field effect transistor (FET)-based biosensor is a non-labeled, rapid and quantitative method to detect ionic or biomolecular charges.[13] The principle of FET has been expected to be applied as a highly sensitive biosensor because of its detection mechanism by which small charge variations of biomolecules can be amplified as the voltage shift at the surface of gate electrode. In the previous works, in which PBA derivatives have been modified and functionalized for FET devices, PBA-coupled FET devices with AlGaN/GaN heterostructures and a PBA-copolymerized gel-based FET were developed for saccharide sensing.[14] Especially, the extended-gate FET allows the selection of various kinds of materials or structures as the gate electrode because the sensing site can be separated from a segment of semiconductor.[15] In the present study, 4-mercaptophenylboronic acid self-assembled monolayer (MPBA–SAM) was formed by the interaction between Au and thiol group on the surface of Au extended-gate as shown in Figure 1a. We report the fundamental electrical properties of PBA–FET biosensor for various saccharide sensing, focusing on the surface properties of MPBA–SAM-coated Au gate electrode and the affinity of PBA with various saccharides.

2. Results and Discussion

2.1. Evaluation of MPBA–SAM on Au Gate Surface

To fabricate the PBA–FET biosensor, MPBA was synthesized by the Au–thiol self-assembly method as a saccharide recognition membrane. The sputtered Au surface was cleaned by UV ozone and immediately immersed in 1 mM MPBA/ethanol solution, so as not to be contaminated by airborne organic compounds. The successful and stable formation of MPBA was checked by contact-angle measurement and ellipsometric analysis. The result of the contact-angle measurement showed that the water static contact angle was $54.8 \pm 0.6^\circ$ for the MPBA–SAM formed on the Au substrate, but $86.5 \pm 1.1^\circ$ for the Au substrate that was treated by UV ozone and immersed in ethanol without MPBA for the same time as the MPBA–SAM treatment, as shown in Figure 2. It is clear that the Au surface treat-

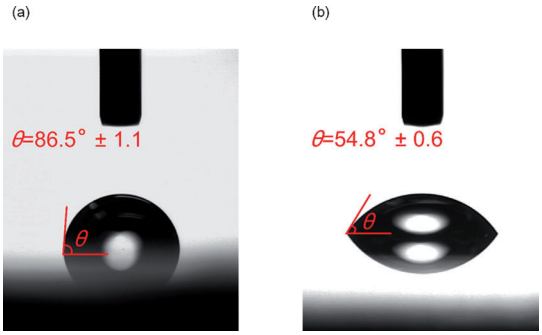

Figure 2. Photographs of dropped water on a) Au surface and b) PBA–SAM treated Au surface. The water contact angles with their standard deviation are shown.

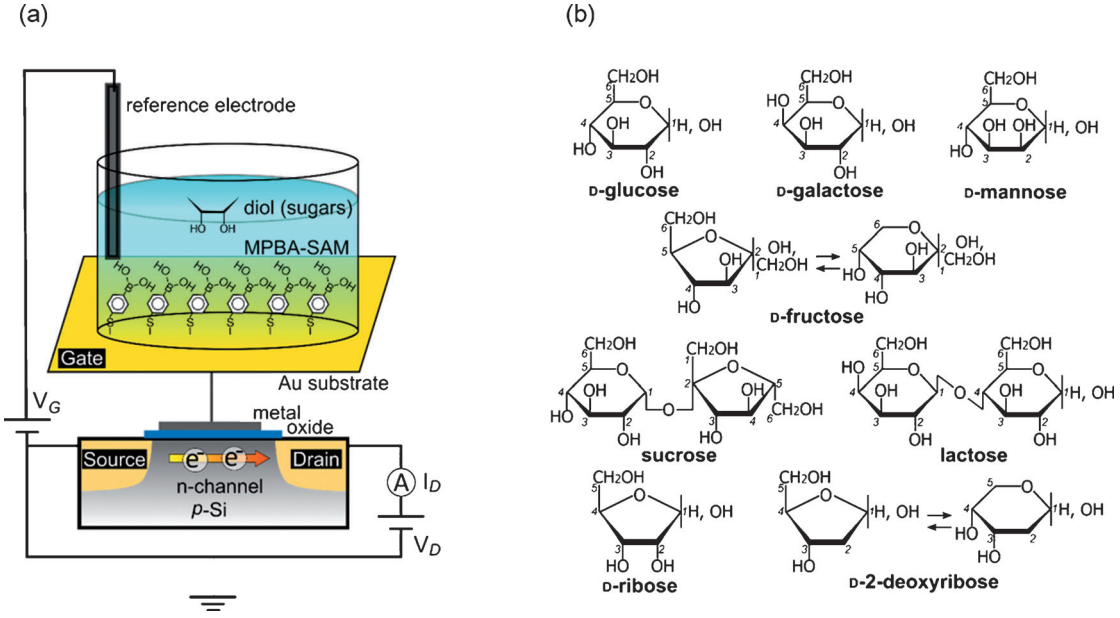

Figure 1. Schematic illustration of PBA–FET structure for sugar recognition. a) Structure of PBA–FET, composed of an extended-gate FET with Au substrate. 4-mercapto-PBA–SAM is chemically tethered to the surface of Au substrate and interacts with diol of sugar. b) Chemical structures of saccharides used in this study. Carbon position number of pyranose and furanose ring noted from reducing-end carbon which is involved with anomerization. Fructose and 2-deoxyribose are depicted as pyranose and furanose conformation according to each equilibrium state in a solution.

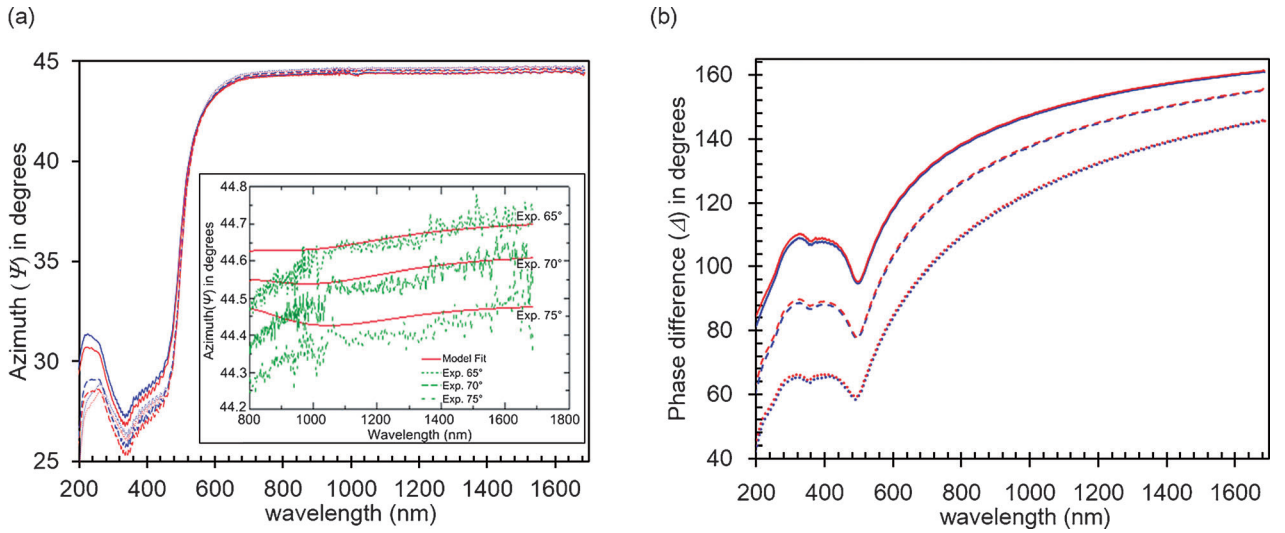

Figure 3. Ellipsometric spectra for Au surface and PBA–SAM-treated Au surface. Blue and red colors are spectra for the Au surface and the PBA–SAM-treated Au surface, respectively. Solid, dashed, and dotted lines corresponded to the spectra of the incidence angles 65°, 70° and 75°, respectively. a) Azimuth (Ψ) spectra of Au surface and PBA–SAM-treated Au surface. The spectra between 800 nm and 1690 nm wavelength are enlarged. In the enlarged figure (inset), green lines indicate experimental spectra of PBA–SAM treated Au surface for each incident light angle, and red lines show model-fitted spectra of each experimental spectra by using WVASE32 software. b) Phase-difference (Δ) spectra of Au surface and PBA–SAM-treated Au surface. The wavelengths of incident light are from 193 nm to 1690 nm, and the angles of incidence are 65°, 70°, and 75°.

ed by MPBA–SAM became hydrophilic even though the value of the contact angle was quite large, as it is known that hydroxyl end-groups turn SAMs superhydrophilic.[16] It was presumed that the hydrophobic surface of the phenyl group affected the contact angle to some extent, but the hydroxyl groups of MPBA were on the outermost surface. The thickness of the MPBA–SAM was calculated by ellipsometric analysis, as shown in Figure 3. Two parameters, Ψ, the azimuth of p- and s-polarized light, and Δ, the phase difference between them, were obtained by the polarization state changes of reflected light from the sample. Compared to the spectra of the unmodified Au surface and the PBA–SAM-treated Au surface, the spectra of the azimuth were obviously changed after the PBA–SAM treatment in Figure 3a, and the spectra of the phase difference were slightly shifted for the PBA–SAM treated Au surface, indicating the thin layer on the Au surface, as shown in Figure 3b. The thickness of the MPBA–SAM was calculated as 1.096 ± 0.094 nm by the Cauchy dispersion model on the assumption of 1 nm of roughness on the Au substrate. The result showed that the MPBA molecules were stably integrated onto the Au surface. Moreover, the adsorption of MPBA on the Au surface was monitored by use of the QCM-D method. Both frequency and dissipation changes are shown in Figure 4. After the introduction of MPBA in the ethanol solution, the frequency decreased drastically and the dissipation increased slightly with thiol–Au binding. From these responses for the MPBA adsorption, the immobilization density of self-assembled MPBA was calculated to be about 0.84 Å^2 per molecule according to the Sauerbrey equation.[17] This result indicates that the density was relatively high but reasonable for SAMs based on thiol–Au binding. On the other hand, the dissipation shift seems to be slight because the MPBA layer was formed as a thin monolayer. These surface properties obtained by the contact angle, the

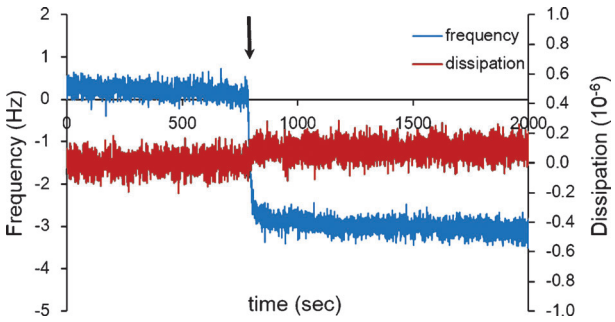

Figure 4. Real-time monitoring of adsorption of MPBA molecules on Au surface using QCM-D. Frequency and dissipation shifts were continuously monitored at room temperature and at flow rates of 100 μL min^{-1} until around 2000 seconds. The result of QCM-D are the normalized frequencies calculated from seventh overtone (35 MHz) for fundamental frequency. The MPBA molecule is introduced in the ethanol solution at the time indicated by the arrow.

ellipsometric and the QCM-D analyses show that the MPBA–SAM was formed precisely and densely on the Au gate surface, resulting in stable electrical signals of FET biosensor caused by the diol binding with saccharides.

2.2. Potential Response for Saccharide Recognition Using PBA–FET Biosensor

The detection principle of a FET sensor is based on the potentiometric detection of charge density changes at the gate electrode, on which specific binding between target and probe molecules is made for molecular recognition. Basically, ionic or molecular charges at the gate interact electrostatically with electrons in silicon crystal through the thin gate insulator and

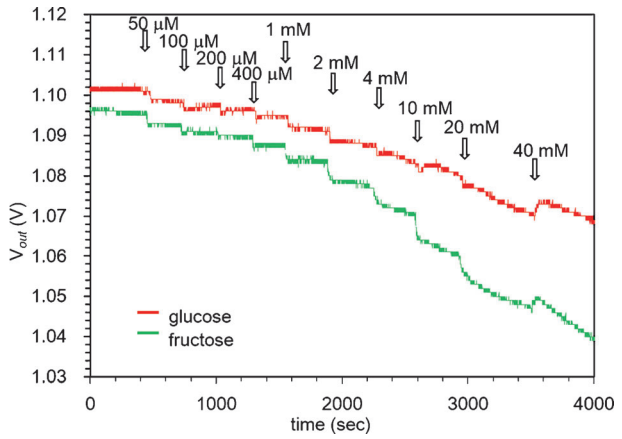

Figure 5. Time course of gate voltage for addition of monosaccharides in the range of 50 μM to 40 mM concentration at room temperature. Red for glucose and green for fructose. At the arrowed points, the sample solutions were introduced onto the PBA–FET.

induce electrical signals by the field effect, resulting in a V_{out} change at constant I_D (Figure 1a). The time course of V_{out} for the diol binding of saccharides with PBA was investigated in a phosphate-buffered saline (PBS) solution (pH 7.4) using the PBA–FET biosensors. Figure 5 shows the time course of V_{out} for the monosaccharides glucose and fructose. The final concentrations of each saccharide were increased from 50 μM to 40 mM in a step-by-step manner. The results indicate that the V_{out} shifted in the negative direction by about 10 mV at most in a staircase pattern between 50 μM to 20 mM for either monosaccharide. This is because the PBA molecule at the quarternary state (state 4 in Scheme 1) based on the diol binding was negatively charged on the surface of Au gate electrode, resulting in the depression of V_{out} at constant I_D. However, an irregular phenomenon was observed at a higher concentration of 40 mM. V_{out} changed inversely in the positive direction upon adding glucose and fructose (40 mM). It is surmised that the equilibrium of PBA–diol binding was transferred from the quarternary to the tertiary state (state 3 or 1 in Scheme 1) due to the excess amount of saccharide substrates. Ayyub et al. reported about fructose detection using a block copolymer film containing PBA, which induced unexpected signals in wavelength shifts at higher concentrations of not only fructose, but also glucose.[18]

The number of ion charges could be calculated from the surface potential changes using the PBA–FET biosensor. The interaction between the glucose molecules and the PBA electrode could be directly transduced into the electrical signal using the FET device. The change in surface charge density could be detected as the surface potential shift of the FET. The surface potential shift after the binding of glucose molecules with PBA molecules, ΔV_{FET}, is expressed in Equation (1), where $\Delta Q_{glu-PBA}$ is the charge per unit area of the charged PBA membrane, and C_i is the gate capacitance per unit area:

$$\Delta V_{FET} = \Delta Q_{glu-PBA}/C_i \quad (1)$$

Since $\Delta V_{FET} = 10$ mV for the binding of glucose with PBA and $C_i = 4.3\times10^{-4}\,F\,m^{-2}$ for the FET, the amount of charges increasing after glucose–PBA binding on the Au electrode was calculated as $4.3\times10^{-6}\,C\,m^{-2}$. As a result of that, the amount of diol binding of glucose-PBA was calculated as 2.7×10^{9} charges cm^{-2}, because the diol binding would induce the increase of a negative charge in a PBA molecule based on the equilibrium reaction (state 4 in Scheme 1). The estimated amount of PBA by the FET was lower than that by the QCM-D analysis. This is because the charged PBA molecules were based on the equilibrium reaction so that all of immobilized PBA molecules were not recognized using the FET biosensor. On the other hand, the QCM-D sensor would have detected the mass change of PBA molecules totally immobilized on the Au substrate regardless of molecular charges. Actually, the measurement experiments were performed in a solution of pH 7.4. Considering that the pK_a of the equilibrium between stages 1 and 2 shown in Scheme 1 is 8.8, most of the PBA molecules modified on the gate surface would not be ionized at a pH of 7.4.[19] Additionally, the equilibrium reaction shifts from stage 1 to stage 4 through stage 3 after the introduction of glucose, resulting in an increase of charged PBA molecules based on the diol binding. However, the amount of ionized PBA molecules would still be small at a pH of 7.4 (lower than the pK_a of 8.8). Therefore, the number of reacted molecules based on the surface potential change using the FET principle would have been calculated as smaller than that of PBA–SAM estimated by use of the QCM-D sensor.

Figure 6 shows the relation between gate voltage shift (ΔV) and logarithm of sugar concentration, in which the straight-line approximations were drawn so that the coefficient of determination (R^2) became the maximum value possible in the range of 50 μM to 20 mM. These experiments were repeated at least three times against each saccharide. As monosaccharides, glucose and its epimer, galactose and mannose, were used to start. Fructose was used as furanose, which is a typical saccharide in the food industry. Sucrose and lactose were used as disaccharides, which are composed of different kinds of monosaccharides: sucrose is represented by β-fructofuranosyl-(2→1)-α-glucopyranoside and lactose by β-D-galactopyranosyl-(1→4)-D-glucopyranoside. Moreover, the components of nucleotide, ribose and deoxyribose were used as furanose as well. In Figure 6, the gradients of the approximation line largely changed at the concentrations of more than 2 mM. In Figure 6a, the relation between ΔV and sugar concentration of four kinds of mono-saccharides such as glucose, galactose, fructose, and mannose, were indicated. The slope of approximate formula and R^2 are shown in Table 1. At up to 2 mM of each saccharide, all the types of saccharide showed similar slopes, between 6.41 and 8.38. On the other hand, a clear difference in slope was found among the four kinds of saccharides at 2 mM to 20 mM. In glucose, almost no change in slope value was found in the range of 50 μM to 20 mM, while the slope value slightly increased for galactose. In fructose and mannose, the linear slopes at more than 2 mM were about three times larger than those at 50 μM to 2 mM. It was considered that the binding mechanism of saccharides to MPBA–

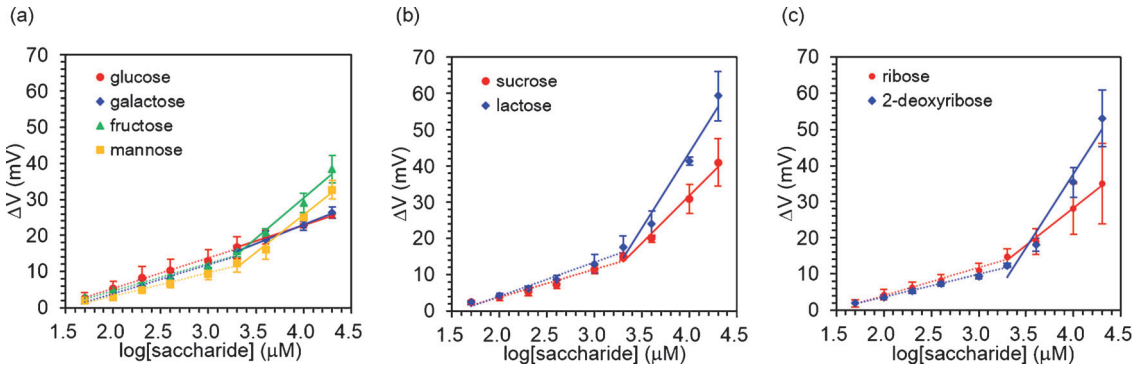

Figure 6. Gate-voltage shift for concentration change of saccharides. a) Potential responses for four kinds of mono-saccharides were investigated for the single logarithmic plots of concentration. b) Potential responses for two kinds of disaccharides were investigated for the single logarithmic plots of concentration. c) Potential responses for two kinds of monosaccharides constituting nucleotides were investigated for the single logarithmic plots of concentration. The approximation line is indicated as a dotted line in the range of 50 μM to 2 mM, and as solid line in the range of 2 mM to 20 mM.

Table 1. Slope and correlation coefficient (R^2) based on approximate formula for potential response in the range of lower or higher sugar concentrations in Figure 6.

Saccharide	Approximate sugar concentration range formula			
	50 μm–2 mm		2 mm–20 mm	
	Slope value	R2	Slope value	R2
glucose	8.38	0.993	8.51	0.997
galactose	8.00	0.970	10.58	0.998
fructose	7.58	0.970	22.43	0.984
mannose	6.41	0.982	20.65	0.983
sucrose	7.77	0.965	26.23	0.984
lactose	9.33	0.971	41.93	0.967
ribose	7.55	0.989	20.65	0.991
2-deoxyroribose	6.25	0.990	41.06	0.964

SAM coated on the Au surface would be different at different sugar concentrations. At above 2 mM sugar concentration, fructose and mannose has higher affinities to PBA compared to glucose and galactose using the PBA–FET. This result is confirmed by earlier reports by Springsteen and Wang[12] and by Ayyub et al.[18] As they had discussed, the 1,2-*cis*-diol structure in fructose preferentially bonds to two hydroxyl groups of boronic acid without steric barrier. Figure 7 shows the three-dimensional conformation of MPBA (Figure 7a), β-glucose (Figure 7b) and β-mannose (Figure 7c) which were modeled by PyMOL software (DeLano Scientific LLC) from Protein Data Bank (PDB) files with little modification.[20] Structural discrimination between glucose and mannose was found only for the conformation of the hydroxyl group at C2 in spite of the apparent difference for potential response in the range of over 2 mM. Considering the previous report as well,[21] it was expected that two hydroxyl groups in PBA (Figure 7a) form preferentially 1,2-*cis*-diol binding compared with 1,3-*cis*-diol binding for the glucose or mannose structures (Figure 7b or Figure 7c), because the distance of each hydroxyl group in PBA is close to that of the hydroxyl groups in each structure. On that point, the expectation is also valid for the binding mechanism of galactose with PBA. In addition, the anomeric carbon which is located at C1 has an effect on the affinity to PBA. In the case of either the glucose or galactose molecules, the hydroxyl groups

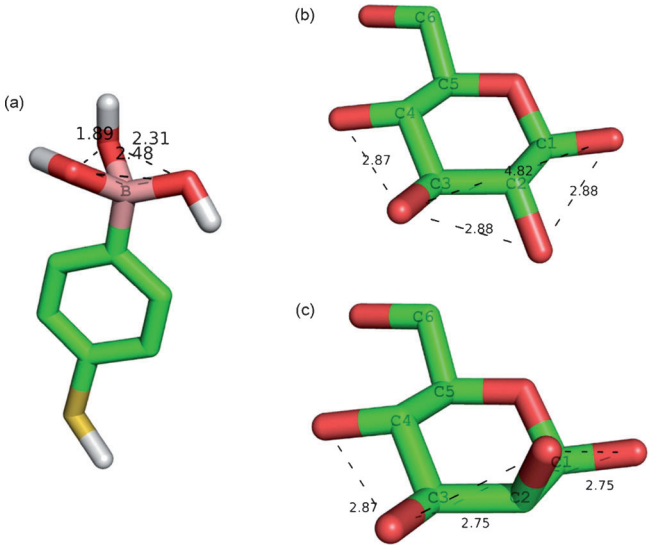

Figure 7. Three-dimensional conformation of 4-mercaptophenylboronic (MPBA) acid (a), β-glucose (b), and β-mannose (c) which were modeled by PyMOL software from PDB files with little modification. Boron atom and carbon numbers correspond to the IUPAC recommendation are indicated such as B and C1 to C6. The distances between each oxygen atom of boronic acid and each hydroxyl group of glucose or mannose were indicated as dotted line.

are alternately formed at C1 so that 1,3-*cis*-diol exists mainly in β-glucose as a major anomer, and the remaining α-glucose forms a 1, 2-*cis*-diol structure.[22] On the other hand, mannose forms a *cis*-diol structure at C2–C3 in either α- or β-mannose, besides doing that at C1–C2 in case of β-mannose, which is formed partially as equilibrium of isomeric form in an aqueous solution.[22] Fructose forms a 1,2-*cis*-diol structure at C1–C2 as a ketose. In aqueous solution, it is known that fructose is mainly formed as β-fructopyranose, and secondarily as β-fructofuranose. In either case, PBA is likely to bind with the 1,2-*cis*-diol of fructose. From these assumptions, the potential response for mannose or fructose is higher than that for glucose and galactose.

Figure 6b shows the evaluation of ΔV evaluated by addition of various amounts of the disaccharides, sucrose and lactose.

The linear slopes for sucrose and lactose recognition using the PBA–FET were 7.77 and 9.33 from 50 μM to 2 mM respectively, and those were quite different at over 2 mM, where they were 26.2 for sucrose and 41.9 for lactose. The slope for lactose recognition was larger than that for sucrose at the higher concentrations. It was possible to consider that the C1 carbon of a unit of glucose in a lactose molecule, which is the more highly reactive aldehyde carbon, remains without the involvement of glycosidic linkage so that the reducing-end of lactose is able to form a diol structure with C2 and act as Lewis base, resulting in the higher affinity to boronic acid as Lewis acid.

Figure 6c shows ΔV for changes in the concentrations of the nucleotides of ribose and 2-deoxyribose, which include the structure of sugar. The linear slopes of ribose and 2-deoxyribose are 7.55 and 6.25 at 50 μM to 2 mM, respectively, while the slopes at over 2 mM increases drastically: 20.6 for ribose and 41.1 for 2-deoxyribose. The potential responses for these nucleotides are similar to those for other sugars at 50 μM to 20 mM. At above 2 mM, the affinity to 2-deoxyribose is higher than that to ribose even though ribose forms a 2,3-*cis*-diol at C2–C3 but a hydroxyl group at C2 was deleted in 2-deoxyribose. This might be because 2-deoxyribose forms 2-deoxyribopyranose as a major isomer, which contains the 3,4-*cis*-diol at the C3–C4 position, so that two hydroxyl groups of boronic acid are able to combine more easily to deoxyribose.[22,23] Moreover, it was predicted that the diol of boronic acid might be likely to interact with the 3,4-*cis*-diol of 2-deoxyribopyranose without the effect of steric hindrance owing to the absence of a hydroxyl group at the C2 position. Thus, the PBA–FET biosensor is expected to realize a simple and highly sensitive detection of the nucleotide substances of DNA, RNA and ATP as well as mono- and disaccharides.

Considering the potential responses for all kinds of monosaccharides within the higher concentration range, the affinity of saccharides with PBA were divided into groups from their slopes of approximate formula (Table 1). In the case of monosaccharides in the range of 2 mM to 20 mM, the slopes of fructose, mannose, and ribose are about 2-fold, and those of 2-deoxyribose about 4-fold greater than those of glucose and galactose. It is considered that the different affinities of saccharides with PBA were caused by factors such as *cis*-conformation of the two hydroxyl groups and distance between them, the ratio of the α/β anomers to the reducing ends, and steric barriers of the hydroxyl groups or axial hydrogens. In particular, the distance between two adjacent hydroxyl groups for *cis*-diol was closer to the distance between hydroxyl groups in PBA than that for *trans*-diol, and that in furanose satisfied more specifically diol-binding with PBA compared to that in pyranose. Moreover, the axial hydrogens, which were bound to each carbon in a sugar ring, would cause steric hindrance and electrostatic repulsion.[18,21,22] It would be possible to identify the specific sugar from the affinity profile using the PBA–FET sensor.

The slopes in the ΔV–sugar-concentration plots for several saccharides were found to change largely at around 2 mM. That reason has not been clarified in detail, but we presumed that the densely packed PBA molecules on the Au electrode would interact with nearby other PBA molecules by oxygen-to-boron binding.[24] That is, the self-binding of PBA on the Au substrate might dissociate depending on the sugar concentration. If the sugar concentrations were less than 2 mM, the attachment of every saccharides to the densely packed PBA layer would cause diol binding based on the equilibrium reaction, but the self-binding of PBA might be kept due to the lower concentration of saccharides, resulting in the reduction of reaction sites. On the other hand, the affinities of diol-binding for each saccharide with PBA molecule should contribute to the electrical signals of PBA–FET biosensor accompanied by the dissociation of self-binding of PBA upon increasing their concentrations more than 2 mM. However, further examination would be needed for clarifying the detection modes on the substrate at the lower concentrations.

In case of glucose sensing, La Belle calculated the limited lowest detection (LLD) and obtained a value of 43.4 μM from the result of experimental measurement in the range of 200 μM to 1 mM using the existing glucose sensor, which was integrated by glucose oxidase and a microfluidic system.[25] In this study, we calculated the detection limit against each saccharide from the single logarithmic plots in the range of 50 μM to 2 mM shown in Figure 6 using the Kaiser limit.[26] Table 2 shows the calculated value of detection limit for each saccharide. Considering the calculated results, the PBA–FET biosensor would have the ability to detect various saccharides at concentrations of more than about 10 μM at least, and in particular allow the detection of glucose at lower concentrations of a few μM. In the case of glucose sensing, the enhancement of the detection limit was expected because of direct detection of molecular charges, without an intervening enzymatic reaction, based on the field effect using the PBA–FET, compared to the improved amperometric and coulometric principle combined with a glass capillary, which enables the detection of 10 μM glucose at 50 °C, and 50 μM glucose at room temperature.[27] Compared to conventional glucose sensors, the sensitivity of the present PBA–FET is closer to the minimum level of sugar concentration. Additionally the device structure is simple without enzyme, but could be further improved by designing device materials, and modifying functional membranes. The

Table 2. Detection limit[a] of PBA-coated gate FET against each saccharide.

Saccharide	Detection limit [μm]
glucose	2.3
galactose	7.0
fructose	7.5
mannose	8.7
sucrose	7.9
lactose	9.8
ribose	2.7
2-deoxyribose	2.6

[a] The detection limit was calculated statistically using Kaiser the limitation from the data of semi-logarithmic plots in the range of 50 μM to 2 mM sugar concentrations in Figure 6.

PBA–FET is able to detect various saccharides electrochemically with high sensitivity regardless of sugar variation so that it would be useful for studying sugar chains consisting of many kinds of saccharides. Therefore, the PBA–FET should be functionalized so as to enhance its specificity at lower sugar concentrations for medical applications such as microbial detection sensors and sugar-chain-recognition sensors. As the surface modification for selective detection, the molecular templated hydrogel was prepared on the gate's sensing surface in order to detect glucose selectively in this paper, particularly. The surface potential changes of PBA–FETs were investigated for the addition of 10 mM glucose and fructose respectively, as shown in Figure 8a and Figure 8b. For each saccharide measurement, the gate surfaces were modified by the glucose-templated hydrogel (Glu-templated gel) or the polymerized hydrogel without glucose (w/o Glu-templated gel), respectively. In the case of the introduction of glucose (Figure 8a), the surface potential of the PBA–FET with the Glu-templated gel shifted by the amount of about 80 mV, which was about five times larger than that for w/o Glu-templated gel. On the other hand, the electrical signal of PBA–FET with the Glu-templated gel was enough smaller (about 40 mV) for the addition of fructose than that of glucose, and additionally the Glu-templated gel-based sensor enabled to suppress the signal for fructose compared to the w/o Glu-templated gel-based one (Figure 8b). The resulted surface potential changes indicated that the Glu-templated gel was effective for the selective detection and the enhancement of affinity of glucose by modifying the gate surface of PBA–FET, although the original PBA–FET showed a higher affinity of fructose with PBA rather than that of glucose (Figure 6). Thus, the molecular-templated hydrogel on the PBA–FET biosensor will be useful for the selective detection of various saccharides in the fields of food engineering and medical application in the future.

3. Conclusions

This paper demonstrated the fundamental electrical characteristics of phenylboronic acid (PBA)-coated gate field effect transistor (FET) biosensor in order to detect directly various saccharides such as monosaccharides (pyranose: glucose, galactose, fructose, and mannose, furanose: ribose and 2-deoxyribose) and disaccharides (sucrose and lactose). The original data in this paper showed two significant facts: 1) the surface properties of a sensing electrode with self-assembled PBA, which were investigated by contact angle, ellipsometer, quartz crystal microbalance (QCM) and FET; 2) the direct and highly sensitive detection of saccharides using the FET with PBA. The specific diol binding of PBA with saccharides induced the molecular charges of PBA, resulting in the detection of charges at a lower concentration of 50 μM based on the principle of field effect. In particular, the binding affinities of PBA with them contributed to the different electrical signals using the PBA–FET biosensor. Moreover, we have found the possibility to induce the selectivity of saccharide sensing by modifying the molecular-templated hydrogel on the PBA–FET gate surface. The platform based on the PBA–FET biosensor is useful for a convenient and highly sensitive detection method of various saccharides in the fields of food engineering and medical applications in the future.

Experimental Section

Materials

The schematic illustration of the structure of PBA–FET is shown in Figure 1a. MPBA was purchased from Sigma–Aldrich (Unite States). The metal oxide semiconductor (MOS)-FET used in this study was an *n*-channel depletion mode FET composed of Si substrate. Monosaccharides: D-glucose, D-galactose, D-fructose, D-mannose, D-ribose, and D-2-deoxyribose; disaccharides: sucrose and lactose were purchased from Wako Pure Chemical Industries, Ltd. (Japan) and their structures were shown in Figure 1b. Ultrapure water (UL Pure, Komatsu Electronics Co., Ltd., Japan) was used in all experiments.

Preparation of Au Gate Electrode with SAM

A gold thin film as the gate electrode was prepared by sputtering (approximately 100 nm thickness), following sputtering Ti film

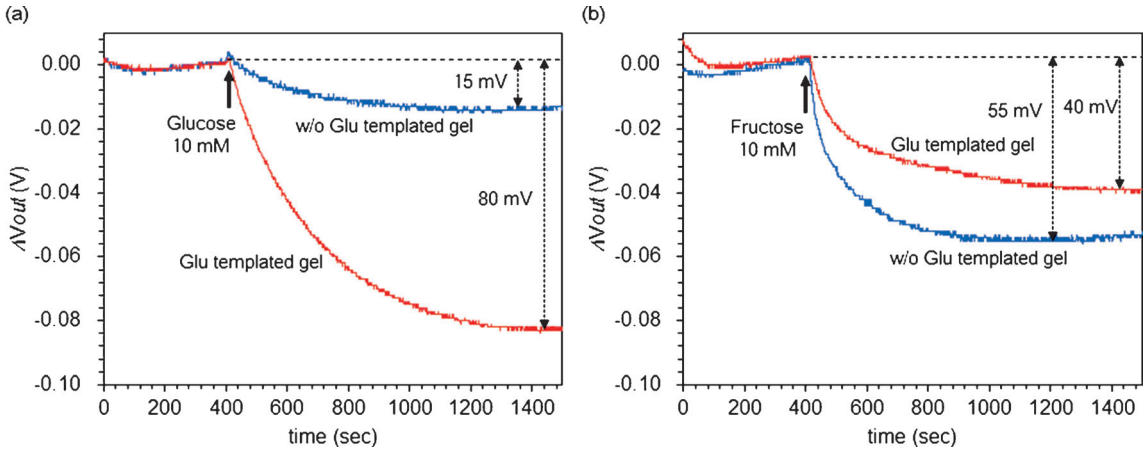

Figure 8. Time course of surface potential change using glucose-templated hydrogel (Glu-templated gel, red line) and polymerized hydrogel without glucose (w/o Glu-templated gel, blue line) for addition of 10 mM glucose (a) and fructose (b).

(approx. 15 nm thickness) on a glass slide (Matsunami Glass Ind., Ltd., Japan). After a polycarbonate ring (18 mm inner diameter/20 mm outer diameter) was encapsulated by the epoxy resin (ZC-203T, Pelnox Ltd., Japan) on the Au surface, the Au surface was treated with MPBA, resulting in the formation of SAM. 1 mM MPBA was diluted with ethanol, in which the Au substrate was immersed after treated by use of UV ozone cleaner (MEIWAFOSIS Co., Ltd., Japan) to remove organic compounds. After the surface treatment for SAM formation, the Au substrates were washed in ethanol twice and in water once and subsequently dried at 110 °C for 1 min.

Measurement of Contact Angle for MPBA–SAM on Au Surface

The formation of SAM was checked by the measurement of static water contact angle using a CA-W automatic contact-angle meter (Kyowa Interface Science, Japan). Ultrapure water drops of 2 μL were placed onto the surface of each sample in an ambient environment. They were monitored using a charge-coupled device (CCD) camera, and the captured images were analyzed using FAMAS software (Kyowa Interface Science) to determine the static contact angle. The contact angle was calculated as the average values based on the images taken ten times at different positions.

Estimation of MPBA–SAM Thickness on Au Surface using the Spectroellipsometric Method

The thickness of the SAM was analyzed by an ellipsometric measurement using a rotating ellipsometer analyzer (model M2000U, J. A. Woollam Co., Inc., U. S. A.) and WVASE32 software. The wavelength of incident light was from 193 to 1690 nm, and the angle of incidence was 65, 70, and 75° for all experiments. For the calculation of layer thickness, the refractive index of the SAM was assumed as 1.50, and considered as the roughness of 1 nm on the Au substrate. The ellipsometric analysis was capable to measure thin films between 0.1 and 1000 nm thickness on the basis of 0.1 nm of a typical sample. To create the most realistic model for the sample, the optical properties of the Au substrate, which was immersed in ethanol without MPBA, were measured after handling in the same way as the samples.

QCM-D Analysis for MPBA–SAM on Au Surface

The QCM sensors used in this study were 14 mm diameter discs, and optically polished AT-cut quartz crystals with Au coating (10 mm diameter) on both sides. The sensors operated at a fundamental frequency of 4.95 (f_0) MHz. The frequency at multiple overtones was measured simultaneously. In this study, the results shown were the normalized frequencies calculated from the seventh overtone ($f_7/7$). Before the measurement, the measurement solution of ethanol was passed through the QCM flow module for 30 min to obtain a stable baseline. MPBA molecules were solved in ethanol.

Real-Time Monitoring of Saccharide-PBA Binding Using Extended-Gate FET

The electrical properties of the extended Au gate FET biosensor was measured by a real-time monitoring analyzer. The PBS (phosphate buffer saline) buffer (pH 7.4) of 1.5 mL was poured into the SAM/Au gate surface equipped with a polycarbonate ring of 20 mm diameter, and equilibrated until the gate surface voltage was stabilized. After the stabilization of surface voltage in the PBS buffer, the sample solutions were gradually added to become from 50 μM to 40 mM in a total volume of several hundred μL. In order to remove the effect of sample addition on the electrical signal, the introduced volume was determined as 1/100 against the whole volume of measurement solution. The time course of the surface potential at the Au gate surface was monitored using the custom-made potential analyzer (GFS-301–4CH, Radiance Ware, Japan). The surface potential (V_{out}) was monitored at a gate voltage (V_G) of 1 V and a drain–source current (I_D) of 700 μA using the circuit used in the previous work.[15]

Molecular-Templated Hydrogel for Selective Detection of PBA-Coated Gate FET

Hydrogel was copolymerized on the Au gate surface coated by the PBA–SAM. Monomer solution was prepared including 0.1 g of 2-hydroxyethylmethacrylate (HEMA, MW = 130.14), 0.05 g of *N*-3-(dimethylamino)propylmethacrylamide (DMAPM, MW = 170.25), 0.005 g of *N*,*N*-methylenebisacrylamide (MBA, MW = 154.17) and 300 μL of 6.7% (wt/wt) acrylic acid solution (AA, MW = 72.06, neutralized with 1 M NaOH as pH 7.4), and weighed up to 1 g by 100 mM sodium phosphate buffer (pH 10.0). In case of fabricating the glucose-templated hydrogel, 0.009 g of glucose was added to the monomer solution. Polymerization was initiated by addition of 2 μL of tetramethylethylenediamine (TEMED) and 5 μL of potassium persulfate (KPS) solution (50 mg mL^{-1}). 10 μL of monomer solution containing or without glucose were poured by pipette on the PBA–SAM-coated Au gate surface which was equilibrated by 50 mM glucose solution (pH 9.0), and a PET coverslip was placed on the monomer solution without air bubble. The gel formation was conducted overnight at room temperature under a nitrogen atmosphere. After gel formation, the coverslip was gently peeled off and washed by 0.1 M HCl/methanol solution for removing template glucose. Before real-time monitoring measurement, the gel was equilibrated with immersing in 100 mM sodium phosphate buffer (pH 9.0) overnight. The electrical property of the FET biosensor was measured by the real-time monitoring analyzer described above. The 100 mM sodium phosphate buffer (pH 9.0) of 1.5 mL was poured on the developed hydrogel in the glass ring well. After the stabilization of surface voltage in the buffer, 15 μL of 1 M glucose or fructose was added in the well controlling the final concentration (10 mM), respectively. The amount of surface potential shift was evaluated for each saccharide with the improved PBA–FET biosensor.

Acknowledgement

The authors wish to thank Dr. K. Konishi of Research Hub for Advanced Nano Characterization, the University of Tokyo in Japan for his help in ellipsometric experiment. A part of this study was supported by Program for Creating STart-ups from Advanced Research and Technology (START program) promoted by Ministry of Education, Culture, Sports, Science and Technology, Japan. The authors declare no competing financial interest.

Keywords: field-effect transistors · glucose · phenylboronic acid · saccharides · sensors

[1] a) J. Sacchettini, L. G. Baum, C. F. Brewer, *Biochemistry* **2001**, *40*, 3009–3015; b) S. Hakomori, *Glycoconjugate J.* **2004**, *21*, 125–137.
[2] J. Davidek, A. W. Khan, *J. Food Sci.* **1967**, *32*, 155–157.

[3] T. W. Siegel, S. R. Smith, C. A. Ellery, J. R. Williamson, P. J. Oates, *Anal. Biochem.* **2000**, *280*, 329 – 331.
[4] Z. L. Chen, D. B. Hibbert, *J. Chromatogr. A* **1997**, *766*, 27 – 33.
[5] a) D. T. Fu, R. A. Oneill, *Anal. Biochem.* **1995**, *227*, 377 – 384; b) H. Kwon, J. Kim, *Anal. Biochem.* **1993**, *215*, 243 – 252; c) K. R. Anumula, *Anal. Biochem.* **1994**, *220*, 275 – 283.
[6] a) Y. B. Vassilyev, O. A. Khazova, N. N. Nikolaeva, *J. Electroanal. Chem.* **1985**, *196*, 105 – 125; b) B. Beden, F. Largeaud, K. B. Kokoh, C. Lamy, *Electrochim. Acta* **1996**, *41*, 701 – 709; c) I. T. Bae, E. Yeager, X. Xing, C. C. Liu, *J. Electroanal. Chem.* **1991**, *309*, 131 – 145; d) M. W. Hsiao, R. R. Adzic, E. B. Yeager, *J. Electrochem. Soc.* **1996**, *143*, 759 – 767; e) R. R. Adzic, M. W. Hsiao, E. B. Yeager, *J. Electroanal. Chem.* **1989**, *260*, 475 – 485.
[7] a) C. J. Davis, P. T. Lewis, M. E. McCarroll, R. Cueto, R. M. Strongin, *Org. Lett.* **1999**, *1*, 331 – 334; b) K. Koumoto, S. Shinkai, *Chem. Lett.* **2000**, *2*, 856 – 857.
[8] a) S. Gao, W. Wang, B. Wang, *Bioorg. Chem.* **2001**, *29*, 308 – 320; b) N. DiCesare, J. R. Lakowicz, *Tetrahedron Lett.* **2002**, *43*, 2615 – 2618; c) J. N. Camara, J. T. Suri, F. E. Cappuccio, R. A. Wessling, B. Singaram, *Tetrahedron Lett.* **2002**, *43*, 1139 – 1141; d) D. B. Cordes, A. Miller, S. Gamsey, Z. Sharret, P. Thoniyot, R. Wessling, B. Singaram, *Org. Biomol. Chem.* **2005**, *3*, 1708 – 1713.
[9] a) T. Kimura, M. Kakeuchi, T. Nagasaki, S. Shinkai, *Tetrahedron Lett.* **1995**, *36*, 559 – 562; b) M. Takeuchi, T. Mizuno, S. Shinkai, S. Shirakami, T. Itoh, *Tetrahedron: Asymmetry* **2000**, *11*, 3311 – 3322.
[10] a) M. Lee, T. Kim, K. Kim, J. Kim, M. Choi, H. Choi, K. Koh, *Anal. Biochem.* **2002**, *310*, 163 – 170; b) N. Soh, M. Sonezaki, T. Imato, *Electroanalysis* **2003**, *15*, 1281 – 1290; c) Y. Ben-Amram, M. Riskin, I. Willner, *Analyst* **2010**, *135*, 2952 – 2959.
[11] S. A. Barker, A. K. Chopro, B. W. Hatt, P. J. Somers, *Carbohydr. Res.* **1973**, *26*, 33 – 40.
[12] a) G. Springsteen, B. Wang, *Tetrahedron* **2002**, *58*, 5291 – 5300; b) J. Yan, G. Springsteen, S. Deeter, B. Wang, *Tetrahedron* **2004**, *60*, 11205 – 11209.
[13] a) P. Bergveld, *IEEE Trans. Biomed. Eng.* **1970**, ##*Bm17*, 70 – 71; b) P. Fromherz, A. Offenhausser, T. Vetter, J. Weis, *Science* **1991**, *252*, 1290 – 1293; c) M. Lahav, A. B. Kharitonov, I. Willner, *Chem. Eur. J.* **2001**, *7*, 3992 – 3997; d) T. Sakata, Y. Miyahara, *ChemBioChem* **2005**, *6*, 703 – 710; e) T. Sakata, Y. Miyahara, *Angew. Chem. Int. Ed.* **2006**, *45*, 2225 – 2228; *Angew. Chem.* **2006**, *118*, 2283 – 2286; f) E. Sharon, R. Freeman, I. Willner, *Electroanalysis* **2009**, *21*, 2185 – 2189; g) J. M. Rothberg, W. Hinz, T. M. Rearick, J. Schultz, W. Mileski, M. Davey, J. H. Leamon, K. Johnson, J. Milgrew, M. Edwards, J. Hoon, J. F. Simons, D. Marran, J. W. Myers, J. F. Davidson, A. Branting, J. R. Nobile, B. P. Puc, D. Light, T. A. Clark, M. Huber, J. T. Branciforte, I. B. Stoner, S. E. Cawley, M. Lyons, Y. T. Fu, N. Homer, M. Sedova, X. Miao, B. Reed, J. Sabina, E. Feierstein, M. Schorn, M. Alanjary, E. Dimalanta, D. Dressman, R. Kasinskas, T. Sokolsky, J. A. Fidanza, E. Namsaraev, K. J. McKernan, A. Williams, G. T. Roth, J. Bustillo, *Nature* **2011**, *475*, 348 – 352; h) T. Sakata, Y. Miyahara, *Anal. Chem.* **2008**, *80*, 1493 – 1496.
[14] a) T. A. Schuller, M. Kuball, S. E. Flower, T. D. James, J. S. Fossey, D. Marcon, J. Das, S. Degroot, M. Germain, A. Sarua, *Sens. Actuators B* **2011**, *160*, 1078 – 1081; b) A. Matsumoto, N. Sato, T. Sakata, K. Kataoka, Y. Miyahara, *J. Solid State Electrochem.* **2009**, *1*, 165 – 170.
[15] T. Sakata, S. Matsumoto, Y. Nakajima, Y. Miyahara, *Jpn. J. Appl. Phys.* **2005**, *44*, 2860 – 2863.
[16] I. Hirata, M. Akamatsu, E. Fujii, S. Poolthong, M. Okazaki, *Dent. Mater. J.* **2010**, *29*, 438 – 445.
[17] G. Sauerbrey, *Z. Phys.* **1959**, *155*, 206 – 222.
[18] O. B. Ayyub, M. B. Ibrahim, R. M. Briber, P. Kofinas, *Biosens. Bioelectron.* **2013**, *46*, 124 – 129.
[19] a) G. E. K. Branch, D. L. Yabroff, B. Bettman, *J. Am. Chem. Soc.* **1934**, *56*, 937 – 941; b) S. Soundararajan, M. Badawi, C. M. Kohlrust, J. H. Hageman, *Anal. Biochem.* **1989**, *178*, 125 – 134.
[20] W. L. DeLano, **2002**, The PyMOL Molecular Graphics System.
[21] S. J. Angyal, D. Greeves, V. A. Pickles, *Carbohydr. Res.* **1974**, *35*, 165 – 173.
[22] F. Franks, *Pure Appl. Chem.* **1987**, *59*, 1189 – 1202.
[23] G. C. Levy, D. J. Craik, Y. Chou, *Nucleic Acids Res.* **1982**, *19*, 6067 – 6083.
[24] D. Barriet, C. M. Yam, O. E. Shmakova, A. C. Jamison, T. R. Lee, *Langmuir* **2007**, *23*, 8866 – 8875.
[25] J. T. La Belle, D. K. Bishop, S. R. Vossler, D. R. Patel, C. B. Cook, *J. Dispersion Sci. Technol.* **2010**, *4*, 307 – 311.
[26] H. Kaiser, *Spectrochim. Acta* **1947**, *3*, 40 – 67.
[27] B. Peng, J. Lu, A. S. Balijepalli, T. C. Major, B. E. Cohan, M. E. Meyerhoff, *Biosens. Bioelectron.* **2013**, *49*, 204 – 209.

Received: June 16, 2014
Revised: August 5, 2014
Published online on September 1, 2014